

TRANSPORT PHENOMENA IN STRATIFIED MULTI-FLUID FLOW IN THE PRESENCE AND ABSENCE OF GRAVITY

Norman Chigier and William Humphrey
Carnegie Mellon University
5000 Forbes Avenue
Pittsburgh, Pennsylvania 15213

ABSTRACT

Experiments are being conducted to study the effects of buoyancy on planar density-stratified shear flows. A wind tunnel to generate planar flows separated by an insulating splitter plate, with either flow heated, which emerge from a two-dimensional nozzle. The objective is to isolate and define the effect of gravity and buoyancy on a stratified shear layer. To this end, both stably and unstably stratified layers will be investigated. This paper reports on the results of temperature and velocity measurements across the nozzle exit plane and downstream along the nozzle center plane.

INTRODUCTION

The objective of this research is to separate the effects of molecular and turbulent diffusion from the effect of buoyancy in the mixing of two fluid layers. This fundamental phenomenon is encountered in many applications. The use of reduced gravity will allow the elimination of buoyant body forces in a flow which contains density gradients.

Transport processes in multi-fluid flows with and without gravity have been studied by several researchers. However, most of these studies concerned themselves with the initiation of convection and diffusion in small, bounded fluid volumes initially at rest (e.g., Refs. 1 & 2). These experiments, with forced flows of variable velocity and buoyancy and stable or unstable density stratification, will provide the means to identify the effect of buoyancy on shear flow.

This research will contribute to the understanding of the fundamental processes involved in the mixing of fluids of different densities. The effects of orientation and the sign of the velocity and density gradients on the mixing process can be individually examined. The reduced gravity environment will also allow the isolation of the effect of density gradients on mixing separate from the effect of buoyancy caused by such gradients in earth gravity.

EXPERIMENTAL APPARATUS AND METHODS

The two-dimensional shear layer is generated by a low-velocity facility similar to a wind tunnel. Fig. 1 shows a sketch of the apparatus and Fig 2 shows the nozzle exit dimensions with the coordinate system used in the experiments. The two flow passages in the tunnel are separated by an insulating plate. The air supplies are independently controlled. The temperature of each stream can be controlled by a 7.5 kW coil heater with a feedback control system. Uniform exit velocities are provided by high contraction ratio two-dimensional nozzles.

The insulating splitter plate between the two flow passages is critical to the performance of the system. The plate must minimize both heat transfer between the flows and flow disturbances. Minimum thickness with adequate insulation properties was achieved thanks to Owens-Corning Corporation, who provided prototype vacuum super-insulation panels. These were faired into a smooth plate by lamination with high-temperature castable ceramic. The final 2° wedge in the nozzle section, used to bring the two flows together at the nozzle exit nearly parallel, was formed from Marinite-I.

Each flow passage has an independently regulated air supply. Air supply flow rate limitations only allow exit velocities of up to 2 m/s. The large expansion ratio diffusers allow a low air velocity in the heater section to ensure a uniform temperature downstream.

The density of the air stream is controlled by temperature. Either stream can be heated to produce stable (top heated) or unstable (bottom heated) stratification in the shear layer. The heater output is regulated by an SCR

power controller with feedback provided by a T-type thermocouple and a digital electronic proportional-integral-derivative feedback controller. This system achieves excellent temperature stability of $\pm 2^\circ\text{C}$ at 200°C . The vertical temperature gradient across the plane of the splitter plate (at $z=0$) is approximately $6.5^\circ\text{C}/\text{mm}$. The temperature is nearly uniform (within $\pm 5^\circ\text{C}$) across more than 50% of the width of the nozzle (Fig. 3).

The flows are accelerated to the desired exit velocity by the one-sided high contraction ratio two-dimensional nozzles. The cross-sectional area distribution was chosen to minimize length and, therefore, heat transfer as well as provide highly uniform flow. Excellent uniformity along the vertical axis is achieved (except for the inevitable boundary layers) and the flow across nearly 50% of the width can be considered two-dimensional (Fig. 4).

Temperature measurements are made using 15 fine-wire Type-K thermocouples. The thermocouples are mounted in a linear array which spans the width of the nozzle exit. A traversing mechanism allows the array to be moved vertically and axially.

Velocity measurements are made with a TSI two-component LDV system. Seeding particles generated by an atomizer are introduced into the flow via perforated tubes mounted horizontally across the flow immediately following the flow straighteners. The LDV system is operated in coincidence mode with the receiving optics placed 30° off-axis in a forward scatter arrangement. The LDV system provides mean and fluctuating velocity measurements as well as fluctuation correlations and the Reynolds shear stress. Due to geometric constraints, measurements cannot be made closer than 5 mm from the nozzle exit ($x/H = 0.2$).

RESULTS

In addition to the temperature and velocity maps of the nozzle exit plane, LDV measurements of the shear layer have been made for the unstratified, stably stratified and unstably stratified conditions. Mean and fluctuating components of axial and vertical velocity were measured simultaneously along the centerplane ($y=0$) of the flow. In all experiments to date, the mean velocity of the upper flow was maintained at $u_t = 1$ m/s and the lower flow at $u_b = 0.5$ m/s. In all stratified cases, the mean temperature of the heated flow was maintained at $T = 200^\circ\text{C}$.

Fig. 5 shows the progression of the axial and vertical velocity profiles at progressive downstream locations of $x/H = 0.2, 1, 2$, and 4 , respectively in the unstratified case. At $x/H = 0.2$ (effectively at the nozzle exit) the axial velocity profile shows nearly uniform velocity except for the boundary layers on the nozzle walls and on the splitter plate. The thickness of the central velocity defect is small and the gradient is steep, so the flow approaches the ideal step profile. At the nozzle exit, the vertical velocity has a sign opposite that of the vertical position. This is due to the slight wedge shape of the splitter plate. The maximum value of v is about 4% of the upper stream velocity, u_t , so the flows are essentially parallel. As the flow progresses downstream, the central velocity defect relaxes and the profile broadens due to entrainment.

Fig. 6 shows the progression of the velocity profiles at downstream locations $x/H = 0.2, 1, 2$, and 4 , respectively for the stably stratified case. At $x/H = 0.2$, the axial velocity profile differs little from the unstratified case. The vertical velocity profile shows the effect of buoyancy as the vertical velocity in the upper flow increases, changing sign. The vertical velocity in the lower flow also increases, and this increase is greatest nearest the splitter plate. This is primarily due to heat transfer through the splitter plate and the accompanying thermal boundary layer. The axial velocity profiles demonstrate the same behavior as the unstratified profiles with the exception that the entire profile rises with distance due to the buoyant nature of the upper flow.

Fig. 7 & 8 show the axial and vertical velocity profiles at downstream locations of $x/H = 0.2$ & 1 , and $x/H = 2$, respectively, for the unstably stratified case. The axial velocity is not grossly changed from the previous, stable, case. The vertical velocity profile at the nozzle exit ($x/H = 0.2$) also does not change appreciably from the stably stratified case. However, as the flow moves downstream, the vertical velocity profile quickly moves towards a nearly uniform upward motion. The magnitude of the vertical velocity is also lower overall than in the stably stratified case.

The data in Fig. 7 was collected with the entire flow seeded. Due to decreasing data rates due to sparse seeding as axial distance from the nozzle increases, conditional sampling was explored. In conditional sampling the two streams are each seeded alone. Velocity profiles are measured twice, once for each condition of seeding. Fig. 8

shows the velocity profiles from each case on the same axes. The vertical positions at which data can be collected overlap due to diffusion and mixing of the seeding particles. The axial velocities show some disparity between the conditions of sampling. The mean velocities in each condition do not represent the mean velocity of the flow at the point in question. Rather, they represent the mean velocity of turbulent eddies which carry seeding particles through the probe volume. However, the vertical velocities agree well in this region. The mean vertical velocity observed is the bulk velocity of the entire flow; it is reasonable to expect that the average vertical velocity of fluctuating eddies about the mean vertical velocity would be zero, and thus not appear in the time-averaged data.

CONCLUSIONS

The low speed stratified shear layer wind tunnel has been built and shown to meet all of the performance criteria required. LDV measurements of an unstratified shear layer were made as a baseline for comparison.

LDV measurements in both stably and unstably stratified shear layers have also been made. As expected, the axial mean velocity profiles do not show a significant dependence on the sign of the density gradient beyond the translation of the whole flow. The vertical velocity profile at the nozzle exit shows great dependence on the existence of a density gradient. The downstream vertical velocity profiles do show some dependence on the sign of the density gradient. For the unstably stratified case, the ascent of the mixing layer is less and the vertical velocity is more nearly uniform across the layer.

Further experiments are underway to determine if this effect of density gradient on the vertical velocities is also dependent on the sign of the velocity gradient. In addition, evidence regarding the existence of large scale structures (Refs. 3 & 4) in the layer is being sought. Both LDV data and flow visualization (using laser sheet photography) will be employed. It is expected that the unstably stratified shear layer will not support such organized structures due to the higher level of turbulence generated.

Initial attempts to ascertain the effect of gravity on the buoyant shear layer will be made in the earth-based low velocity facility. The experiment will be arranged so that the gravity vector is perpendicular to the dimensions of interest, by rotating the tunnel about its long axis by 90°.

ACKNOWLEDGMENT

This work was supported by a grant from the NASA Microgravity Science and Applications Division (NASA Grant NAG3-1505).

REFERENCES

1. Koster, J.N. and Sani, R.L. (Ed.), "Low Gravity Fluid Dynamics and Transport Phenomena", Progress in Astronautics and Aeronautics, AIAA, Washington, D.C., Vol. 130, 1990
2. Prakash, A. et al, "Convective Instabilities in a Two-Layer Fluid System", AIAA Paper 91-0313, 1991
3. Brown, G. and Roshko, A., "On the Density Effects and Large Structures in Turbulent Mixing Layers", J. Fluid Mechanics, Vol. 64, pp. 775-816, 1974
4. Chandrsuda, R. et al, "Effects of Free-stream Turbulence on Large Structure in Turbulent Mixing Layers", J. Fluid Mechanics, Vol. 85, pp. 693-704, 1978

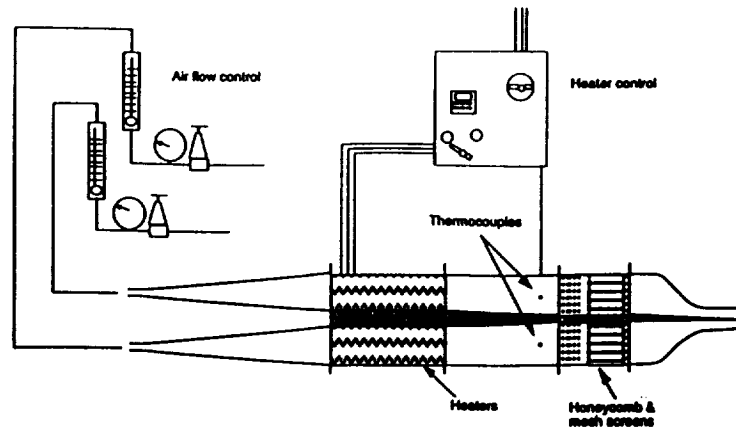


Fig. 1: Two-dimensional Shear Layer Wind Tunnel Schematic

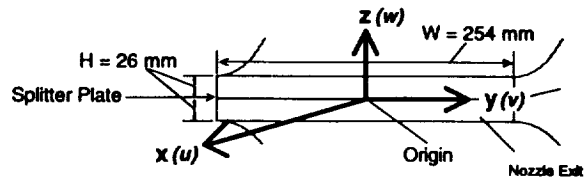


Figure 2: Nozzle Dimensions and Coordinate System

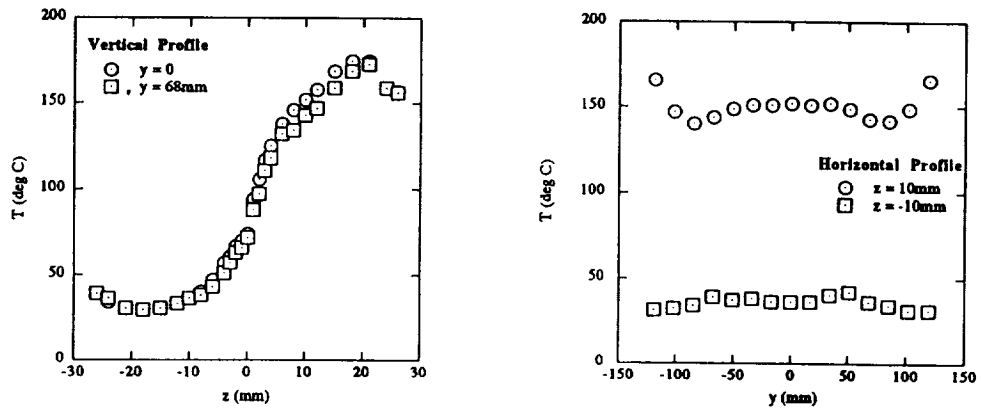


Fig. 3: Nozzle Exit Plane Temperature Profiles (top stream heated to 200°C)

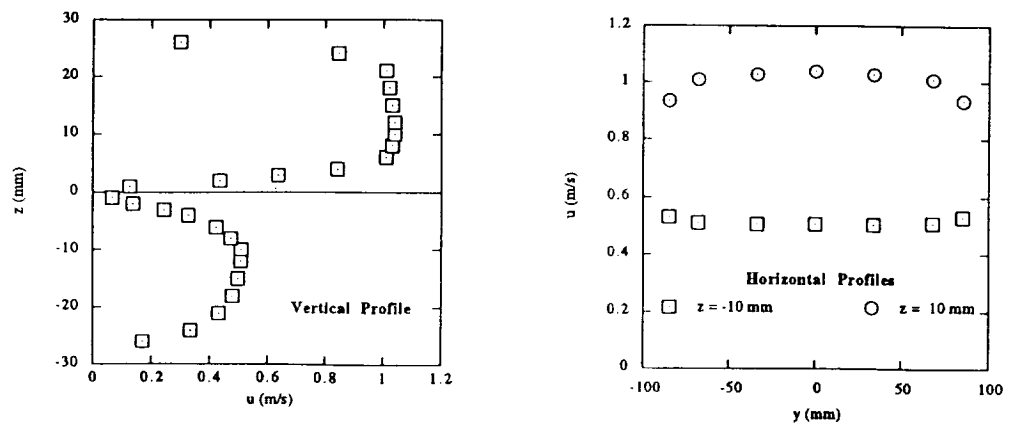


Fig. 4: Nozzle Exit Plane Axial Velocity Profiles (unheated flow)

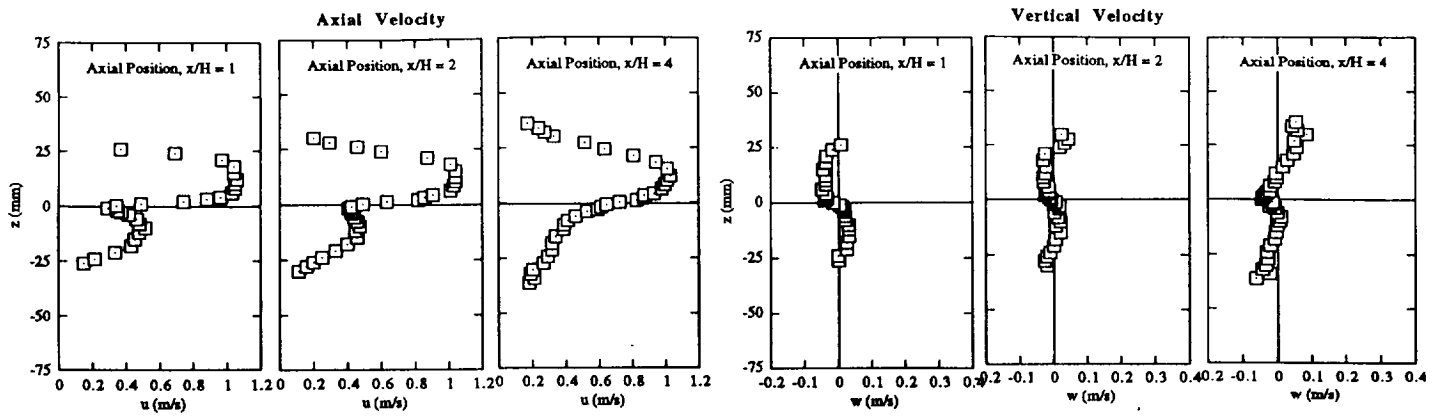


Fig. 5: Downstream Velocity Profiles (unheated flow)

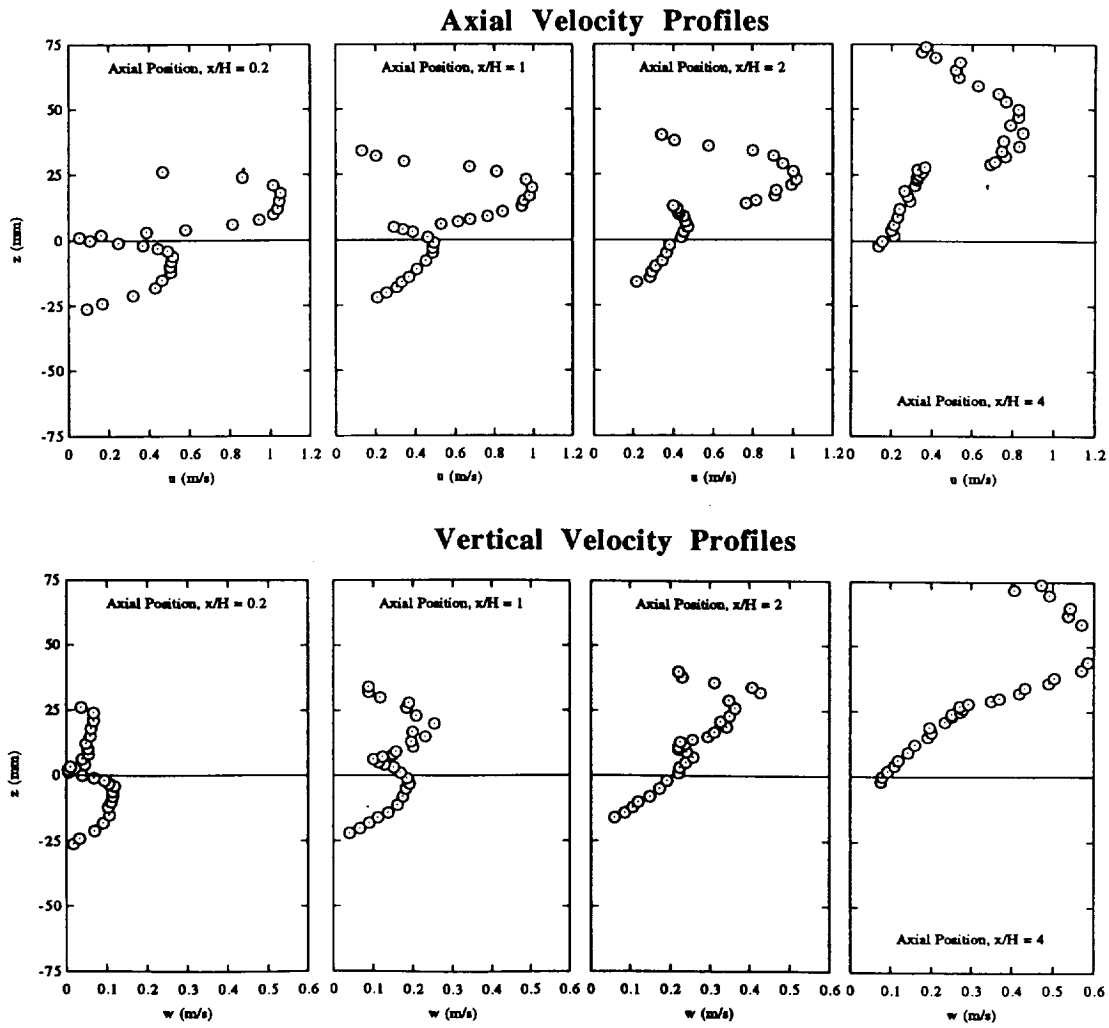


Fig. 6: Velocity Profiles (stably stratified, top stream $T=200^{\circ}\text{C}$)

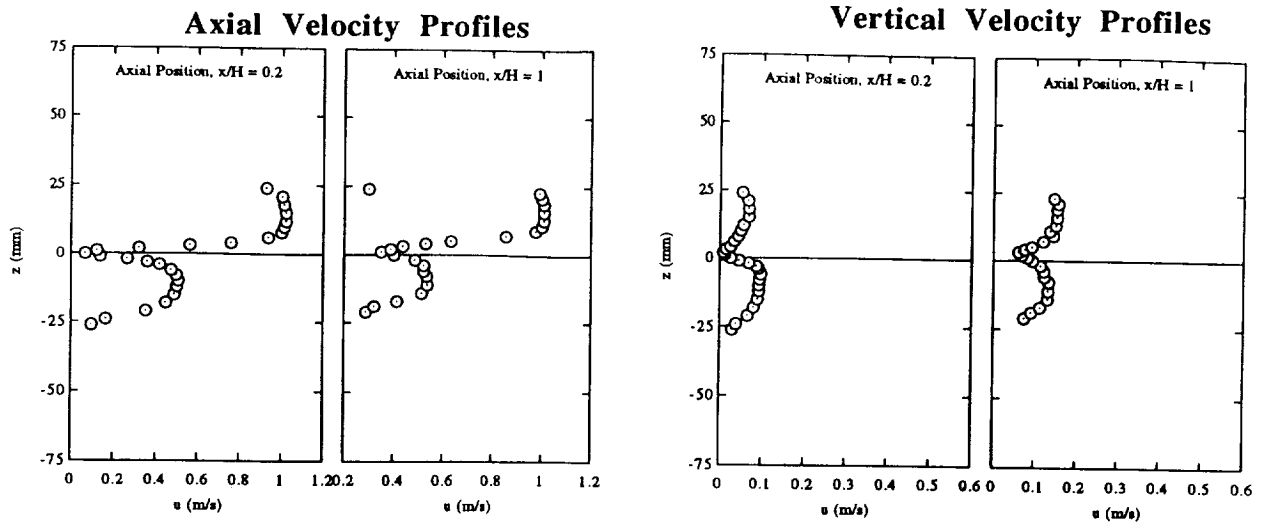
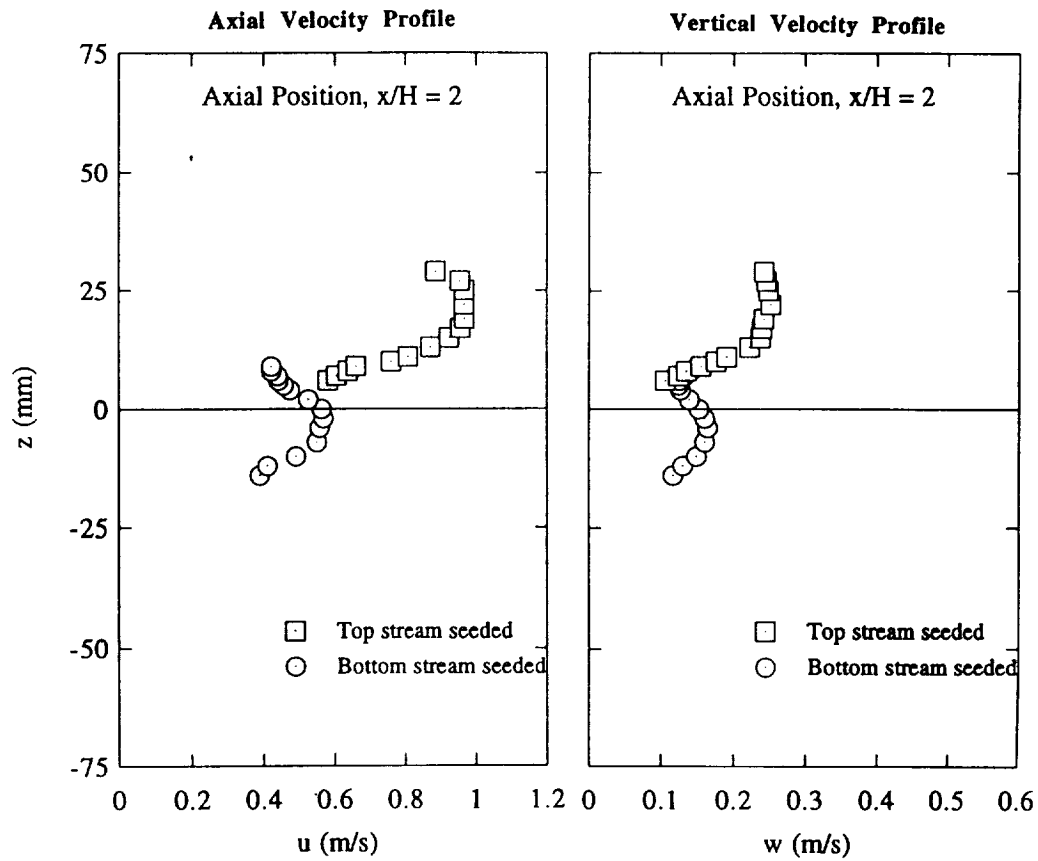


Fig. 7: Velocity Profiles (unstably stratified, bottom stream $T=200^{\circ}\text{C}$)



**Fig. 8: Velocity Profiles (unstably stratified, bottom stream $T=200^{\circ}\text{C}$)
Conditional Sampling**